Nanostructured Copper Filaments in Electrochemical Deposition

Mu Wang,* Sheng Zhong, Xiao-Bo Yin, Jian-Ming Zhu, Ru-Wen Peng, Yuan Wang,
Ke-Qin Zhang, and Nai-Ben Ming

National Laboratory of Solid State Microstructures and Department of Physics, Nanjing University, Nanjing 210093, China
(Received 31 July 2000)

In this Letter we report a novel self-organized copper electrodeposition in an ultrathin layer of $CuSO_4$ electrolyte. The macroscopic fingering branches of the deposit consist of long copper filaments covered with periodic corrugated nanostructures. The mechanism of the nanostructure formation is explored and the origin of the significant descent of the branching rate in electrodeposition is discussed. We suggest that this growth phenomenon provides deeper insights into the role of diffusion and migration on pattern formation in electrodeposition.

DOI: 10.1103/PhysRevLett.86.3827 PACS numbers: 81.15.Pq, 45.70.Qj, 79.60.Jv, 82.80.Fk

Recently electrochemical metallization of copper has been applied for on-chip interconnection in microelectronics [1,2]. With this development, direction-controlled electrodeposition has attracted much attention [3]. To understand and control the deposit formation, it is essential to know the influence of physicochemical environments near the growing interface, for instance, the effect of convection [4–8], on the electrodeposition. It is intriguing to know whether the ramified feature remains when the external agitations are suppressed, and whether regular patterns can be directly electrodeposited. Monte Carlo simulation shows that by changing the strength of electromigration, deposit morphology may vary from fractal to stringy pattern [9]. An experimentally similar tendency is observed in a strong electric field [10,11], where the deposit branches look straight macroscopically, yet on microscopic scale the branches are still ramified due to the diffusive instability. On the other hand, the electrodeposition can be nucleation controlled [12–14], which is sensitive to the variation of the concentration/electric fields at the growing front. Because of the competition of nutrient transport and interfacial kinetics, interfacial concentration field may become unstable [15]. Hence the nucleation rate of metal fluctuates, and the electrodeposition is modulated. In this Letter we report the formation of a unique copper electrodeposit from an ultrathin film system. The macroscopic fingering branch of the deposit consists of long, narrow copper filaments with self-organized periodic nanostructures. The branching rate of the copper deposit is significantly decreased compared to previous reports [13,16]. The chemical compositions along the structured filament are analyzed. The mechanism of this unusual growth behavior is discussed.

The cell for the experiments consists of two clean glass plates, separated 50 μm by spacers. The circular anode (ϕ20 mm) is made of copper wire (99.9%, Goodfellow), and the cathode is a graphite rod (ϕ0.5 mm) inserted through a small hole on the upper glass plate and touching the electrolyte [17]. The electrolyte solution is prepared by analytical reagent $CuSO_4$ and ultrapure water. The concentration is 0.05 M. A Peltier element is placed beneath the cell to reduce temperature and to solidify the electrolyte. $CuSO_4$ is partially expelled from the solid in the solidification due to the partitioning effect. Eventually an ultrathin layer of concentrated $CuSO_4$ electrolyte is formed between the ice of electrolyte and the upper glass plate when equilibrium is reached. The electrodeposit develops in this layer. At -4 °C the layer thickness is about 200 nm, which is estimated from the thickness of the copper deposit measured by atomic force microscope (AFM). The concentration in this trapped layer does not exceed 0.7 M, which is the saturation concentration of $CuSO_4$ at -4 °C. The details of experimental method will be reported separately [17].

After confirming that the potentiostatic and the galvanostatic experiments generate similar deposit morphology, we apply a constant voltage of 4.0 V across the electrodes. The typical copper deposit is shown in Fig. 1(a). Unlike previously reported random branching morphology [13,16], here the deposit branches are fingering and have smooth contour. The deposit is shiny and grows robustly on the glass substrate. Optical microscopy reveals that the fingering branch consists of "cellular structures" [Fig. 1(b)], and each is composed of long, narrow copper filaments. Although unbranched long filaments (more than 150 μm) can be found occasionally, bifurcation occurs to most of them. The overall density of the deposit and the average interfilament separation do not change evidently, so the cellular pattern gradually increases in width. It can be seen from the tip region that the filaments are perpendicular to the contour of the fingering branches, which suggests that the copper filaments develop along the local electric field.

AFM reveals striking periodic corrugated structures on the filaments (Fig. 2). It is noteworthy that the corrugations on the neighboring filaments correlate in position, which can be easily identified in the branch-splitting regions [Fig. 2(b)]. The coherence of these corrugations implies that they were generated simultaneously. The coherent, periodic growth of the filaments is associated with

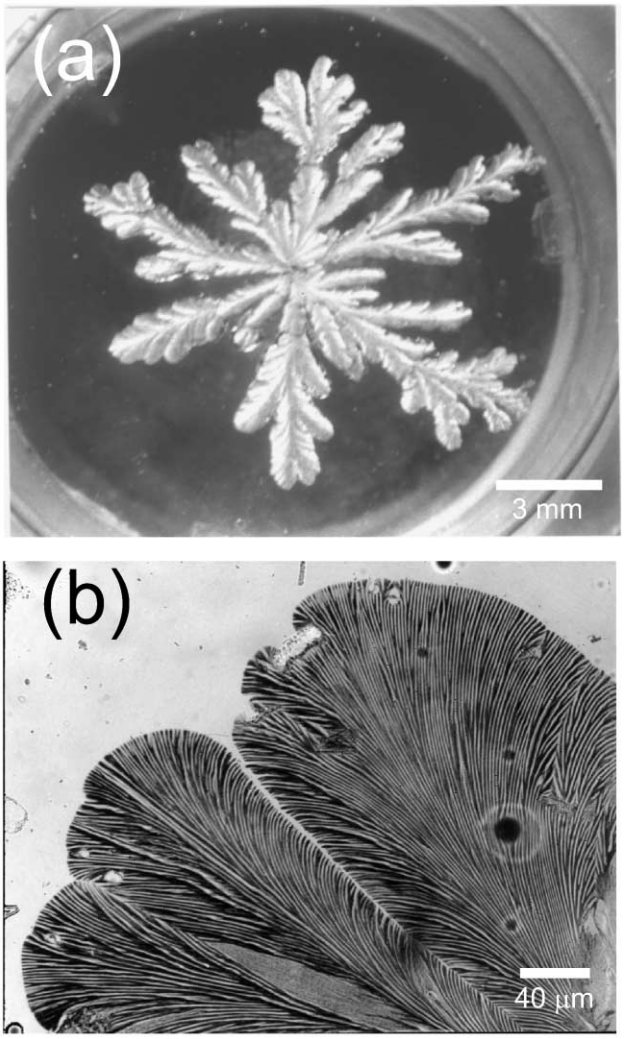

FIG. 1. (a) The fingering electrodeposit grown on a glass substrate from an ultrathin film of $CuSO_4$ solution. (b) The optical micrograph of the fingering branches shown in (a), in which fine filaments can be seen. The fingering branches orient to different directions, so the growth of the filaments is not restricted to the specific orientations. The initial concentration of the electrolyte (C) was 0.05 M, the temperature (T) was -4 °C, and the applied voltage (V) was 4.0 V.

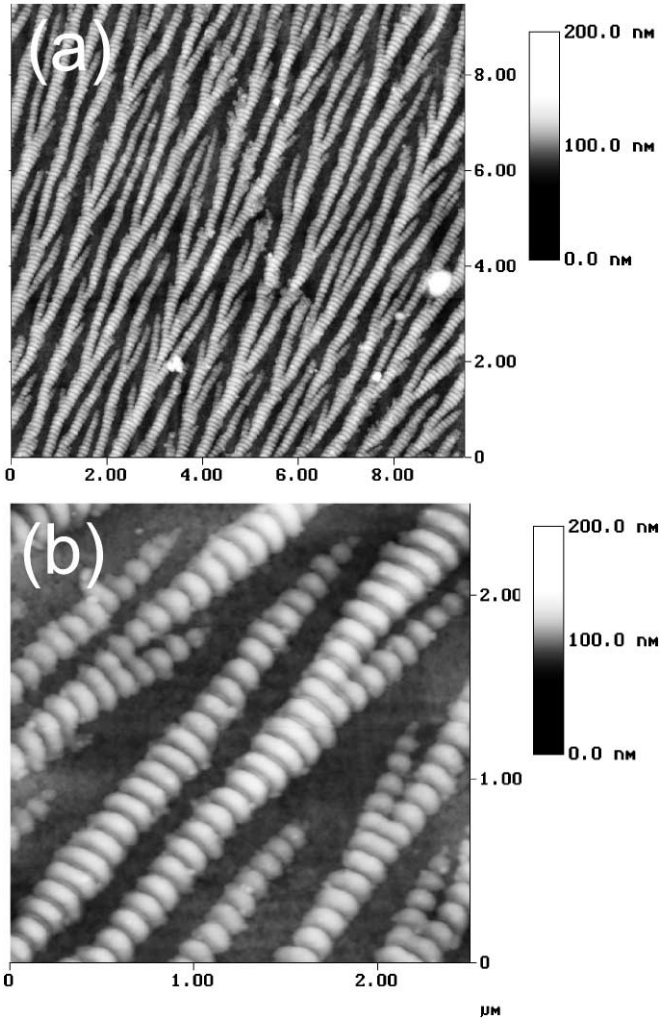

FIG. 2. (a) The copper filaments viewed by AFM (Nanoscope IIIa) with contact mode. The top surface of the filaments is rounded, indicating that it was not confined by any flat, rigid surface during the growth. The corrugated structures can be seen on the copper filaments. (b) The copper filaments viewed with a higher magnification. The periodic corrugations on the neighboring filaments are correlated in position. The parameters for the electrodeposition: $V = 4.0$ V, $T = -5$ °C, pH $= 4.5$.

an evident oscillation of electric current. The period of these spatiotemporal oscillations depends on the voltage across the electrodes, the pH of the electrolyte, and the temperature, etc. Details will be presented in a forthcoming paper [18]. The distinct difference between the electrodeposit shown here and those reported previously [13,16] is that here the branching rate has been significantly decreased, and the surface of the deposit becomes much smoother.

The structure and chemical composition of the corrugated copper filaments have been analyzed by a transmission electron microscope (TEM). Figure 3(a) illustrates the diffraction contrast image of the filaments, where the crystallites within each corrugated structure are a few tens of nanometers in size. The electron diffraction of the copper filament [Fig. 3(b)] confirms that it is polycrystalline. In addition to the diffraction of copper, diffraction of Cu_2O is also identified. Cu_2O is usually abundantly generated in alkali electrolyte or high electrode potential [11,19–21]. In our case where the pH of the electrolyte is 4.5 and the voltage is a few volts, Cu_2O still exists. The electric resistivity of the copper filaments shows, however, that the average concentration of Cu_2O in the filament is less than 2% [17]. We examine the distribution of Cu_2O along a filament by analyzing the diffraction strength at the sites A–F shown in Fig. 3(a). Suppose the orientations of the crystallites in the filament are random. It turns out that the ratio of the integrated strength of the diffraction of $Cu_2O(111)$ versus that of Cu(200), which is proportional to the ratio of the local content of Cu_2O and Cu, fluctuates as a function of position [Fig. 3(c)]. Although the data in Fig. 3(c) are qualitative, they do indicate that the content of

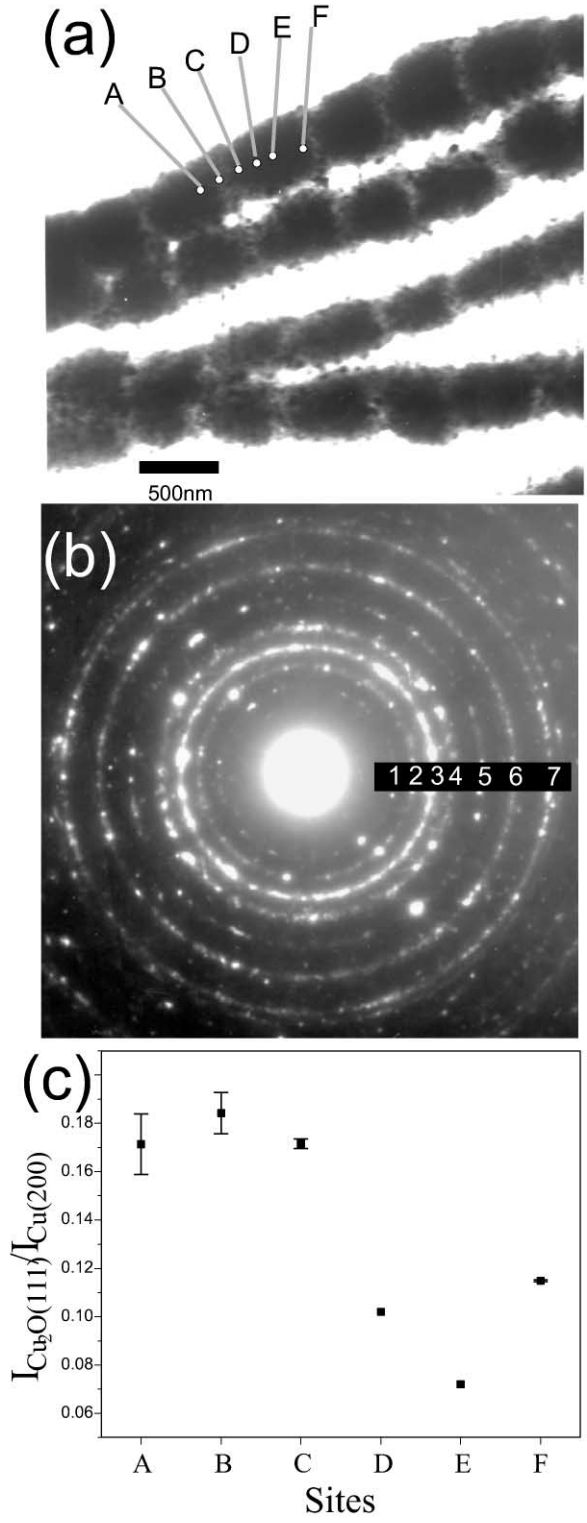

FIG. 3. The TEM (JEM-4000EX) analysis of the corrugated copper filaments. (a) The diffraction contrast image of the filaments. (b) The electron diffraction of the filament. The numbers on the diffraction rings represent the following: (1): Cu_2O (110); (2): Cu_2O (111); (3): Cu (111); (4): Cu (200); (5): Cu_2O (220); (6): Cu (220); (7): Cu (311), respectively. (c) The ratio of the integration strength of the diffraction of $Cu_2O(111)$ vs that of Cu(200) at the sites marked by $A-F$ in (a). The percentage of Cu_2O is higher at the sites B and F. The parameters for the sample preparation: $p\mathrm{H} = 4.5$, $V = 2.5$ V, $T = -2.75\,^{\circ}\mathrm{C}$.

Cu_2O is higher at the sites B and F. This means that indeed the periodic corrugated structure on the copper filament is related to the fluctuation of Cu_2O concentration during the electrodeposition.

Electrocrystallization of copper can be understood as follows: Cu^{2+} ions are driven to the cathode by electric field, then they are reduced and diffuse on the deposit surface. Nucleation of the adsorbed atoms, followed by limited growth, gives rise to a crystallite agglomerate. According to the Nernest equation, the equilibrium electrode potential of $Cu\,|\,Cu^{2+}$ increases when the concentration of Cu^{2+}($[Cu^{2+}]$) builds up. The deposition of copper takes place only when the potential of the cathode is lower than this equilibrium value. The equilibrium electrode potential for Cu_2O, however, is much higher than that for Cu. So for a wide range of the electrolyte concentration Cu_2O deposits with priority. Suppose $[Cu^{2+}]$ is initially high at the growing interface, so the equilibrium potential for copper deposition is also high. By applying a sufficiently low electrode potential, both Cu and Cu_2O are deposited. It should be noted that the deposition rate of Cu_2O is proportional to the product of both $[Cu^{2+}]$ and $[OH^-]$ [20], whereas $[OH^-]$ is much lower than $[Cu^{2+}]$. Therefore, the deposition rate of Cu_2O is very low compared to that of copper. The electrodeposition consumes Cu^{2+}; at the same time the ion transport is confined by the ultrathin electrodeposition system. As the result, $[Cu^{2+}]$ decreases in front of the growing interface, and it takes time for the Laplacian fields to compensate this reduction. Meanwhile the equilibrium electrode potential of Cu decreases and it may even become lower than the actual electrode potential. Once this occurs, copper deposition stops, yet the deposition of Cu_2O remains. Note that Cu_2O grows with a very low rate, which allows $[Cu^{2+}]$ in front of the growing interface to be accumulated again. Consequently the equilibrium electrode potential of Cu^{2+} resumes. When its value exceeds the actual electrode potential, copper deposition restarts. In this way the copper filaments with periodically modulated concentration of Cu_2O, and hence periodic nanostructures are generated.

The crucial difference of our experimental system and previous ones is that the thickness of the electrolyte is decreased to the order of the length of mean free path of ion diffusion [22], which leads to the distinct morphologies shown in Figs. 1 and 2. In the ultrathin film only a small fraction of the cations can move forward without collision with the boundaries. As a matter of fact, the mean free path of ion diffusion in a thin electrolyte film with two rigid boundaries, $\overline{\lambda}$, can be expressed as

$$\frac{1}{\overline{\lambda}} = \frac{1}{\overline{\lambda}_\infty} + \frac{1}{L},$$

where L is the thickness of the electrolyte film and $\overline{\lambda}_\infty$ is the mean free path in a bulk system. As L approaches $\overline{\lambda}_\infty$, $\overline{\lambda}$ decreases evidently. The diffusion constant D is proportional to $\overline{\lambda}$ according to the transport theory. Therefore ion diffusion in an ultrathin layer is slower. The

electromigration, the other factor that contributes to the cation transfer, is driven by the electric field and may not be sensitive to the descent of the film thickness. We expect that the electric migration may overwhelm the diffusion in an ultrathin film electrodeposition. Hence the ballistic deposition plays a more important role than the diffusion-limited growth. This may change the deposit morphology significantly. In electrodeposition the frontmost tips of the copper filaments are the "hot points" for nucleation. According to the theory of Chazalviel [23], the cation concentration behind the growing front virtually approaches zero, which prohibits further nucleation there. These factors ultimately lead to the less-ramified copper filaments. Moreover, suppression of the convective noise may also play a role. The convection caused by the vertical temperature or the concentration gradient can be characterized by Rayleigh number, which relates to the thickness of the solution film d as d^3 [24]. The convection is reduced drastically by decreasing d. For electroconvection, we expect that its strength also declines, although the exact solution for 3D electroconvection is difficult to achieve [25]. In addition, viscosity of the electrolyte also increases at low temperature and high electrolyte concentration, which may affect the deposit morphology. In-depth discussions will be presented elsewhere [18].

It is true that the fingerlike electrodeposit has been reported before [26]. However, the patterns shown here are different from previous ones in many ways. First, the ramification of the deposit has been greatly suppressed, and smooth filaments can be generated on the substrate. Second, periodic nanostructure with periodic variation of chemical compositions is formed, which marks the evolution of the deposit, and helps to understand the mechanism of electrodeposition. Moreover, it has been shown that on a different length scale the factors governing the pattern formation are different. On the scale above the order of the thickness of the concentration boundary layer, the morphology is mainly governed by the Laplacian fields. So the fingering pattern dominates [Fig. 1(a)]. On the scale of the mean free path of ion diffusion, the role of electromigration becomes evident; hence straight filaments appear. By demonstrating the effect of dimensionality of the growth system on electrocrystallization, the phenomena shown here provide deeper insights of pattern formation in electrodeposition.

We acknowledge the support of the National Natural Science Foundation of China and the Ministry of Science and Technology of China. The authors thank Q. Wu, L. Lam, and W. Wang for discussions.

*Electronic address: muwang@netra.nju.edu.cn

[1] D. Edelstein *et al.*, Tech. Dig. Int. Electron. Devices Meet. **1997**, 773 (1997).
[2] S. Venkatesan *et al.*, Tech. Dig. Int. Electron. Devices Meet. **1997**, 769 (1997).
[3] J. C. Bradley *et al.*, Nature (London) **389**, 268 (1997).
[4] V. Fleury, J. Kaufman, and D. B. Hibbert, Nature (London) **367**, 435 (1994).
[5] M. Wang, W. J. P. van Enckevort, N.-B. Ming, and P. Bennema, Nature (London) **367**, 438 (1994).
[6] K.-Q. Zhang *et al.*, Phys. Rev. E **61**, 5512 (2000).
[7] J. Huth *et al.*, Phys. Rev. E **51**, 3444 (1995).
[8] J. R. de Bruyn, Phys. Rev. Lett. **74**, 4843 (1995).
[9] J. Erlebacher, P. C. Searson, and K. Sieradzki, Phys. Rev. Lett. **71**, 3311 (1993).
[10] J. R. Melrose, D. B. Hibbert, and R. C. Ball, Phys. Rev. Lett. **65**, 3009 (1990).
[11] M. Q. Lopez-Salvans, F. Sagues, J. Claret, and J. Bassas, Phys. Rev. E **56**, 6869 (1997).
[12] V. Fleury, Nature (London) **390**, 145 (1997).
[13] V. Fleury, and D. Barkey, Europhys. Lett. **36**, 253 (1996).
[14] S. N. Atchison, R. P. Burford, and D. B. Hibbert, J. Electroanal. Chem. **371**, 137 (1994).
[15] M. Wang *et al.*, Phys. Rev. E **60**, 1901 (1999).
[16] T. Vicsek, *Fractal Growth Phenomena* (World Scientific, Singapore, 1992), 2nd ed., and references therein.
[17] S. Zhong *et al.*, J. Phys. Soc. Jpn. (to be published).
[18] S. Zhong and M. Wang (to be published).
[19] J. A. Switzer *et al.*, J. Am. Chem. Soc. **120**, 3530 (1998).
[20] E. W. Bohannan *et al.*, Langmuir **15**, 813 (1999).
[21] F. Texier, L. Servant, J. L. Bruneel, and F. Argoul, J. Electroanal. Chem. **446**, 189 (1998).
[22] The mean free path of cation diffusion can be estimated by $\lambda = 1/\sqrt{2}\, n\sigma$, where n is the ion concentration, and σ is the cross section of ion scattering. σ is roughly estimated as $\sigma = \pi R^2$, where R is the radius of Cu^{2+}. It follows that the mean free path of the ion transfer is around 300 nm.
[23] J.-N. Chazalviel, Phys. Rev. A **42**, 7355 (1990).
[24] F. Rosenberger, *Fundamentals of Crystal Growth I* (Springer-Verlag, Berlin, 1979).
[25] V. Fleury, M. Rosso, and J.-N. Chazalviel, in *Defect Structure, Morphology and Properties of Deposits*, edited by H. D. Merchant (TMS, Warrendale, PA, 1995), p. 195.
[26] M. Q. Lopez-Salvans *et al.*, Phys. Rev. Lett. **76**, 4062 (1996).